Electroweak corrections to dilepton production at LHC: the Drell–Yan process vs the Photon Fusion mechanism

V. A. Zykunov (JINR, GSU)

The XV-th International School-Conference
"The Actual Problems of Microworld Physics"
Minsk, Belarus, 27 August – 3 Sept., 2023

Introduction

Despite the fact that the Standard Model (SM) keeps for oneself the status of consistent and experimentally confirmed theory, the search of New Physics (NP) manifestations is continued:

- ⋆ **the supersymmetry**,
- ⋆ **M-theory**,
- ⋆ **DM-particles**,
- ⋆ **axions**,
- ⋆ **feebly interacting particles**,
- ⋆ **extra** spatial dimensions,
- ⋆ **extra** neutral gauge bosons, etc.

One of powerful tool in the modern experiments at LHC is the investigation of **Drell–Yan dilepton production**

$$pp \to \gamma, Z \to l^+ l^- X \tag{1}$$

at **large invariant mass** of lepton pair: $M \geq 1$ TeV.

Drell-Yan process (1970, BNL)

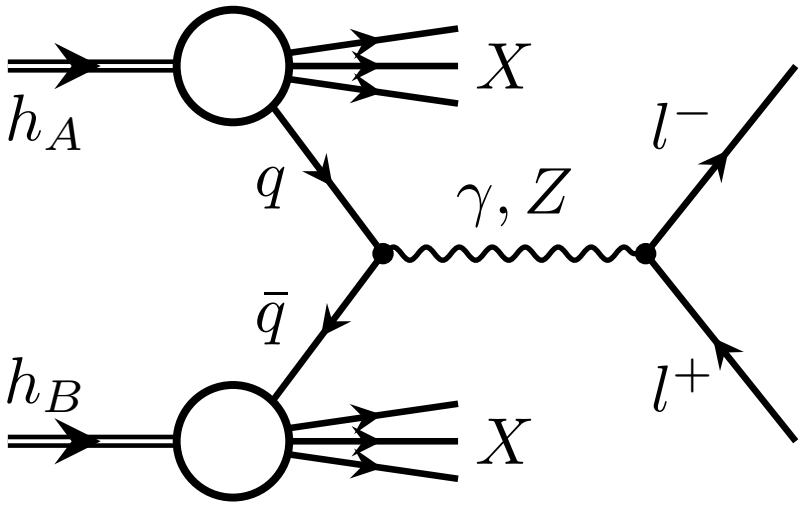

Figure 1: Drell-Yan process with neutral current

- ★ $\sqrt{S}$ is total energy in c.m.s. of hadrons
- ★ M is dilepton l^+l^- invariant mass ($l = e, \mu$)
- ★ y is dilepton rapidity

Current experimental situation at CMS LHC

★ The measured Drell–Yan cross sections and forward-backward asymmetries are consistent with the SM predictions at

$$\sqrt{S} = 7\text{–}8 \text{ TeV } (19.7 \text{ fb}^{-1}) \text{ for } M \leq 2 \text{ TeV},$$
$$\sqrt{S} = 13 \text{ TeV } (85 \text{ fb}^{-1}) \text{ for } M \leq 3 \text{ TeV}$$

- ★ differential cross section $\frac{d\sigma}{dM}$,
- ★ double-differential cross section $\frac{d^2\sigma}{dMdy}$,
- ★ forward-backward asymmetry A_{FB}.

★ NNLO RCs are taken into account by using of **FEWZ**,

★ NNLO PDFs are **CT10 NNLO** and **NNPDF2.1**.

Some modern codes for NLO and NNLO RC for DY process at hadronic colliders (in the ABC order)

- ⋆ DYNNLO (S. Catani, L. Cieri, G. Ferrera et al.)
- ⋆ FEWZ (R. Gavin, Y. Li, F. Petriello, S. Quackenbush)
- ⋆ HORACE (C.Carloni Calame, G.Montagna, et al.)
- ⋆ MC@NLO (S. Frixione, F. Stoeckli, P. Torrielli et al.)
- ⋆ PHOTOS (N. Davidson, T. Przedzinski, Z. Was et al.)
- ⋆ POWHEG (L. Barze, G. Montagna, P. Nason et al.)
- ⋆ RADY (S. Dittmaier, A. Huss, C. Schwinn et al.)
- ⋆ READY (V. Zykunov, RDMS CMS)
- ⋆ SANC (Dubna: A. Andonov, A. Arbuzov, D. Bardin et al.)
- ⋆ WINHAC (W. Placzek, S. Jadach, M. W. Krasny et al.)
- ⋆ WZGRAD (U. Baur, W. Hollik, D. Wackeroth et al.)

Code READY and a set of prescriptions

In the following the scale of radiative corrections and their effect on the observables of Drell–Yan processes will be discussed using FORTRAN program **READY**: (**R**adiative corr**E**ctions to l**A**rge invariant mass **D**rell–**Y**an process).

We used the following set of prescriptions:

- ⋆ standard PDG set of SM input electroweak parameters,
- ⋆ "effective" quark masses ($\Delta\alpha_{had}^{(5)}(m_Z^2) = 0.0276$),
- ⋆ 5 active flavors of quarks in proton,
- ⋆ CTEQ, CT10, and MHHT14 sets of PDFs,
- ⋆ choice for PDFs: $Q = M_{sc} = M$.

CMS detector setup

We impose the experimental restriction conditions

- ★ on the detected lepton angle $-\zeta^* \leq \cos\theta \leq \zeta^*$ (or on the rapidity $|y(l)| \leq y(l)^*$); for CMS detector the cut values of ζ^* (or $y(l)^*$) are determined as

$$\zeta^* \approx 0.986614 \quad (\text{or} \;\; y(l)^* = 2.5),$$

- ★ the second standard CMS restriction $p_T(l) \geq 20$ GeV,
- ★ the "bare" setup for muon identification requirements (no smearing, no recombination of muon and photon/gluon).

Mathematical Content

At the edges of kinematical region (extra large $\sqrt{S}$, M) the important task is make the RC procedure both accurate and fast. For the latter it is desirable to obtain **the set of compact formulas** for the EWK and QCD RCs.

Leading effect of **Weak RCs** in the region of large M is described by the Sudakov Logarithms (**SL; V. Sudakov, 1956**):

$$\log \frac{m_B^2}{|r|} \quad (B = Z, W; \quad r = s, t, u). \tag{2}$$

Collinear Logarithms (**CL**) play leading role in description of **QED RCs and QCD RCs**:

$$\log \frac{m_f^2}{|r|} \quad (f = e, \mu, q; \quad r = s, t, u). \tag{3}$$

Notations, invariants, coupling constants

The standard set of **Mandelstam invariants** for the partonic elastic scattering:

$$s = (p_1 + p_2)^2, \quad t = (p_1 - k_1)^2, \quad u = (k_1 - p_2)^2. \tag{4}$$

The propagator for j-boson depends on its mass and width:

$$D^{js} = \frac{1}{s - m_j^2 + i m_j \Gamma_j}. \tag{5}$$

Suitable combinations of coupling constants are:

$$\lambda_f{}_+^{i,j} = v_f^i v_f^j + a_f^i a_f^j, \quad \lambda_f{}_-^{i,j} = v_f^i a_f^j + a_f^i v_f^j, \tag{6}$$

$$v_f^\gamma = -Q_f, \quad a_f^\gamma = 0, \quad v_f^Z = \frac{I_f^3 - 2 s_W^2 Q_f}{2 s_W c_W}, \quad a_f^Z = \frac{I_f^3}{2 s_W c_W}.$$

Main features of EWK and QCD RCs calculation

The notations, the Feynman rules and renomalization detailes are inspired by review of **M. Böhm, H. Spiesberger, and W. Hollik, 1986**:

- ⋆ **the t'Hooft–Feynman gauge**,
- ⋆ **on-mass renormalization scheme** ($\alpha, \alpha_s, m_W, m_Z, m_H$ and the fermion masses as independent parameters),
- ⋆ **ultrarelativistic approximation**.

QCD result can be obtained from QED case by substitution:

$$Q_q^2\alpha \to \sum_{a=1}^{N^2-1} t^a t^a \alpha_s = \frac{N^2-1}{2N} I\alpha_s \to \frac{4}{3}\alpha_s, \tag{7}$$

here $2t^a$ – Gell-Man matrices, and $N = 3$.

Two mechanisms: DY and $\gamma\gamma$-fusion

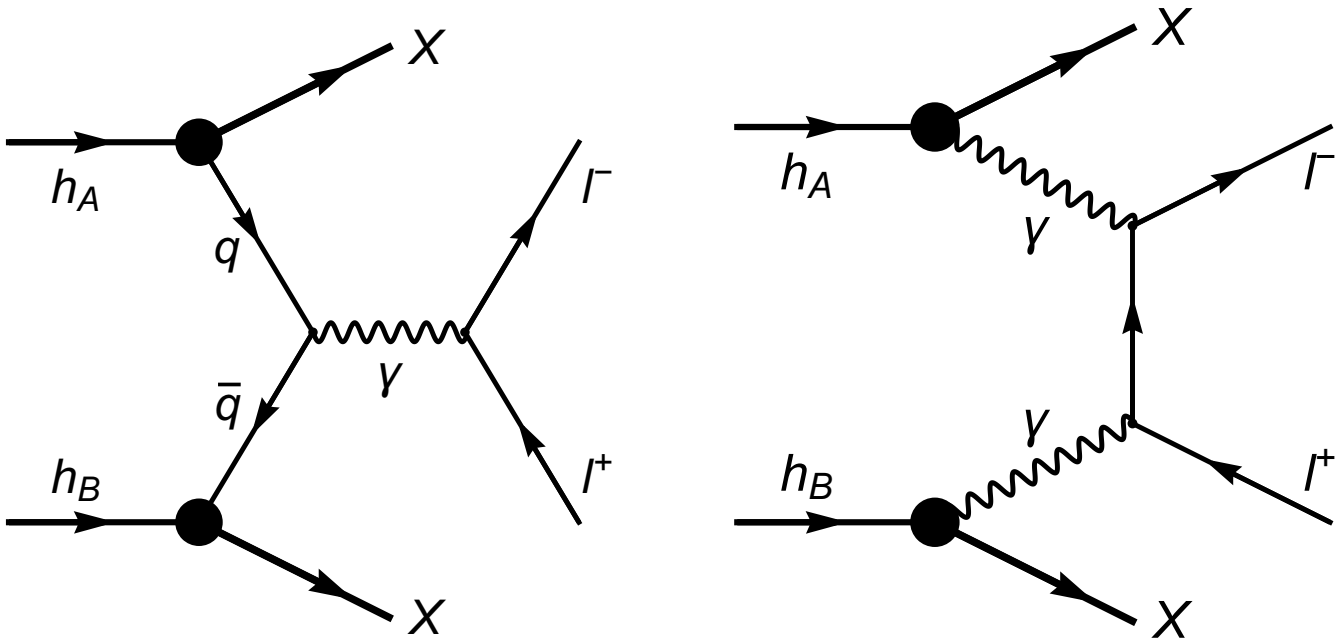

Figure 2: Dilepton production in hadron collisions: left – the Drell–Yan process with virtual photon, right – the photon-photon fusion.

$\gamma\gamma$-fusion Born: diagrams and cross sections

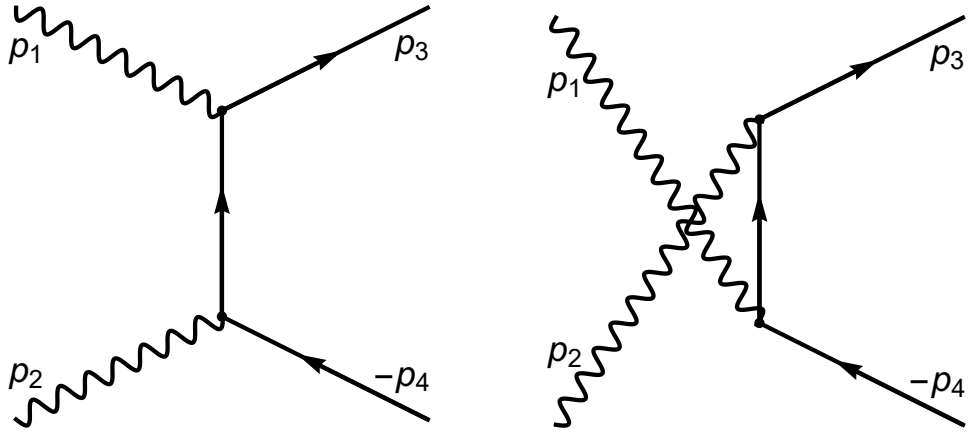

Figure 3: Feynman diagrams of $\gamma\gamma \to l^- l^+$ process at Born level.

Parton level:

$$d\sigma_0^{\gamma\gamma} = \frac{2\pi\alpha^2}{s^2}\frac{t^2+u^2}{tu}dt. \tag{8}$$

Hadron level ($\mathcal{C} = \cos\theta$):

$$\frac{d^3\sigma_0^h}{dMdyd\mathcal{C}} = 8\pi\alpha^2 f_\gamma^A(x_1) f_\gamma^B(x_2)\frac{t^2+u^2}{SM^5(1-\mathcal{C}^2)}\Theta. \tag{9}$$

DY vs $\gamma\gamma$: diff. cross section $d\sigma/dM$

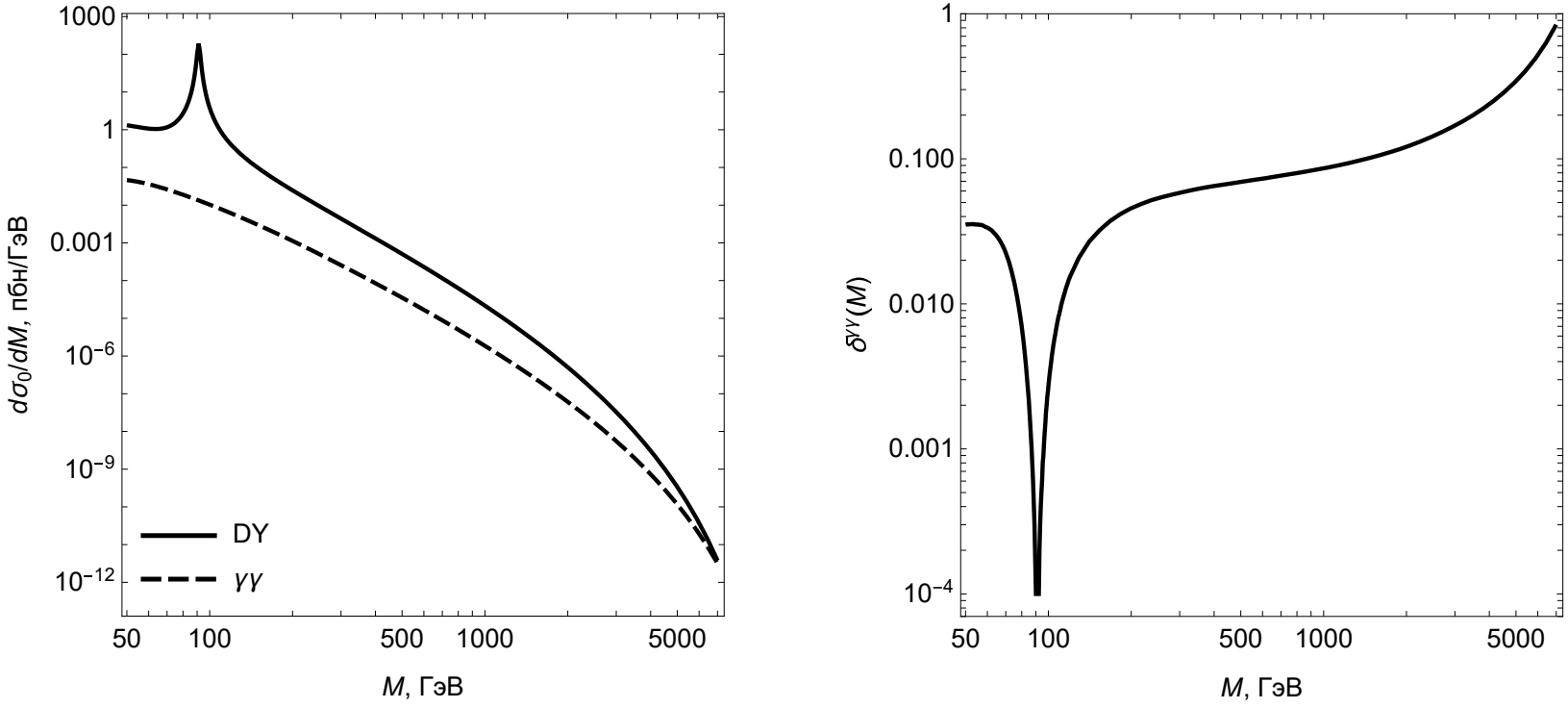

Figure 4: Left – differential Born cross section via M, right – the relative correction $\delta^{\gamma\gamma}(M)$ via M:

$$\delta^{\gamma\gamma}(M) = \frac{d\sigma_0^{\gamma\gamma}/dM}{d\sigma_0^{\mathrm{DY}}/dM}. \tag{10}$$

DY vs $\gamma\gamma$: double diff. cross section $d^2\sigma/dMdy$

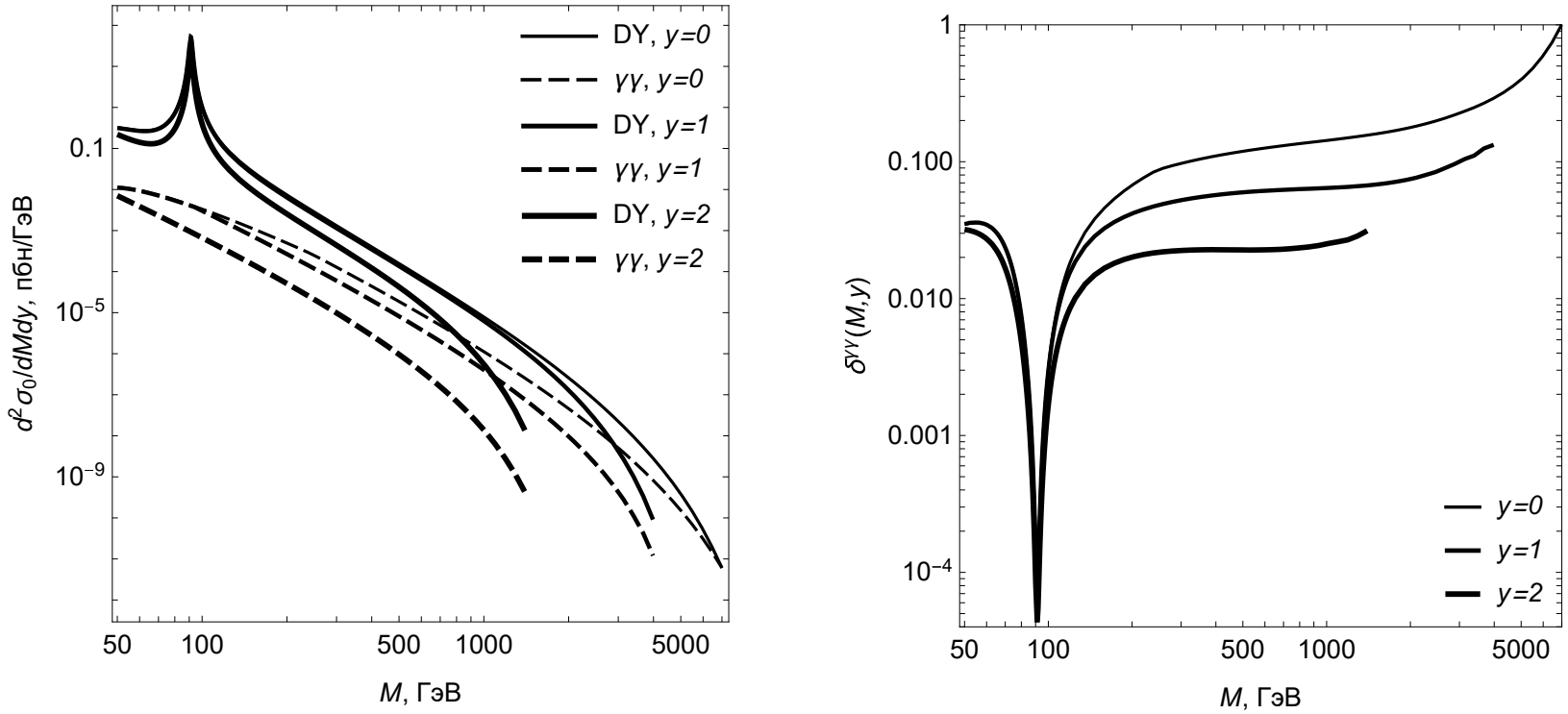

Figure 5: Left – double differential cross sections via M at different y. right – the relative corrections $\delta^{\gamma\gamma}(M, y)$ via M at different y.

Virtual diagrams: γ and Z

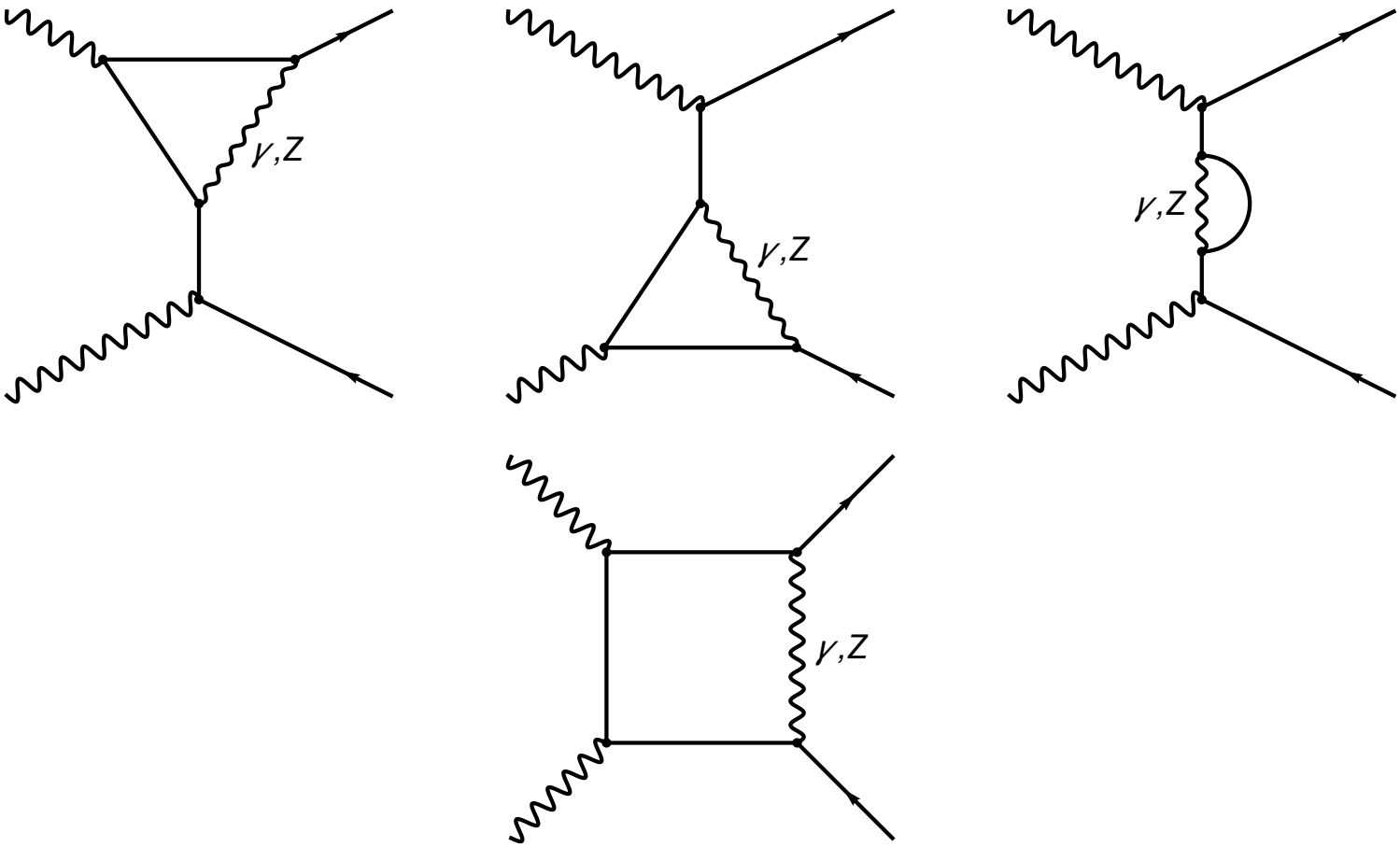

Figure 6: Half of Feynman diagrams set for $\gamma\gamma \to l^- l^+$ process with additional virtual γ and Z-boson: vertices, electron self energies, boxes. The rest diagrams are obtained by $p_1 \leftrightarrow p_2$.

Virtual diagrams: W

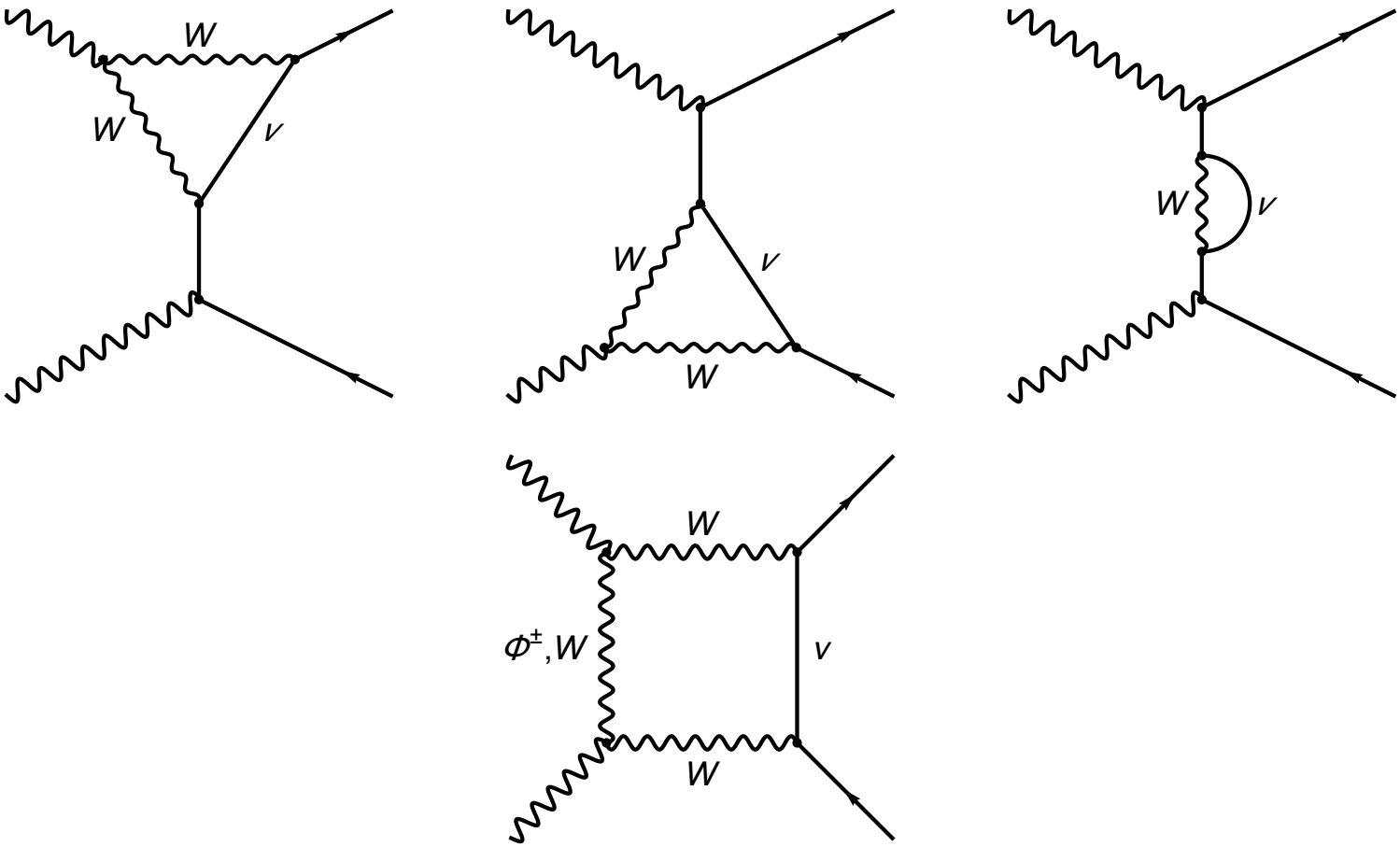

Figure 7: Half of Feynman diagrams set for $\gamma\gamma \to l^- l^+$ process with additional virtual W-boson: vertices, electron self energies, boxes. The rest diagrams are obtained by $p_1 \leftrightarrow p_2$.

Bremshtrahlung diagrams

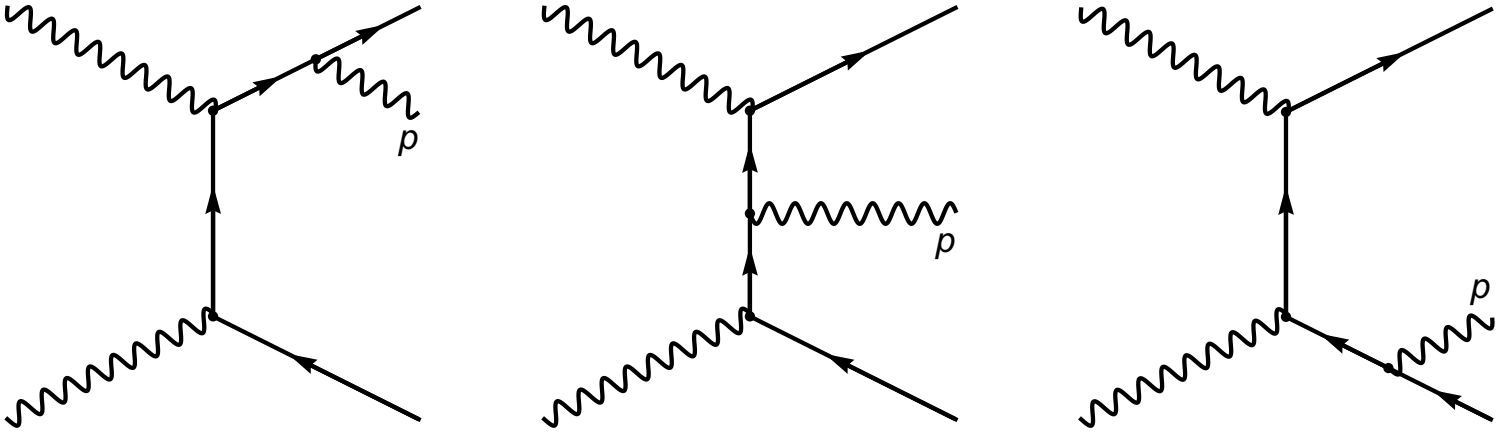

Figure 8: Half of Feynman diagrams set for $\gamma\gamma \to l^- l^+ \gamma$ process. The rest diagrams are obtained by $p_1 \leftrightarrow p_2$.

Virtual + soft contribution

The virtual and soft contributions are factorized before Born cross section **(M. Böhm and T. Sack, 1986)**:

$$\delta_{\rm QED} = \frac{\alpha}{\pi}\Big(\log\frac{4\omega^2}{s}(L-1) + \frac{\pi^2}{3} - \frac{3}{2} + \frac{tu}{t^2+u^2}[f(t,u)+f(u,t)]\Big),$$

where the function

$$f(t,u) = \frac{s^2+t^2}{2tu}L_{st}^2 - \frac{3u}{2t}LL_{st} - L_{st}.$$

is entering in the cross section symmetrically (with $t \leftrightarrow u$), and the **collinear "big" log** and **angle log** look like:

$$L = \log\frac{s}{m^2}, \quad L_{st} = \log\frac{s}{-t}. \tag{11}$$

Weak contributions: Z and W

The **weak corrections** are factorized too:

$$\delta_Z = -\frac{\alpha}{\pi}(v_Z^2 + a_Z^2)\frac{tu}{t^2+u^2}\big[G_Z(t,u) + G_Z(u,t)\big],$$

$$\delta_W = -\frac{\alpha}{\pi}\frac{1}{4s_W^2}\frac{tu}{t^2+u^2}\big[G_W(t,u) + G_W(u,t)\big].$$

Assuming the **HE asymptotic** $\sqrt{s} \gg m_Z$ we get:

$$G_Z^{\rm HE}(t,u) = \frac{t^3 L_{st}^2}{2u^3} + \frac{tL_{tZ}}{2u}(L_{sZ}+L_{st}-1) - \frac{tL_{sZ}}{u} - \frac{t^2 L_{st}}{u^2} + \frac{t(27-2\pi^2)}{12u},$$

$$G_W^{\rm HE}(t,u) = \frac{t^2}{su}\left(\pi^2 - L_{sW}^2\right) + \frac{t}{u}\left(\frac{\pi^2}{3} + L_{tW}^2\right) - \frac{3u}{2t}L_{tW} - L_{st} + \frac{5u}{4t},$$

where **Sudakov logs** look like:

$$L_{tB} = \log\frac{-t}{m_B^2}, \quad L_{sB} = \log\frac{s}{m_B^2}; \quad B = Z, W.$$

Independance of unphysical parameter ω

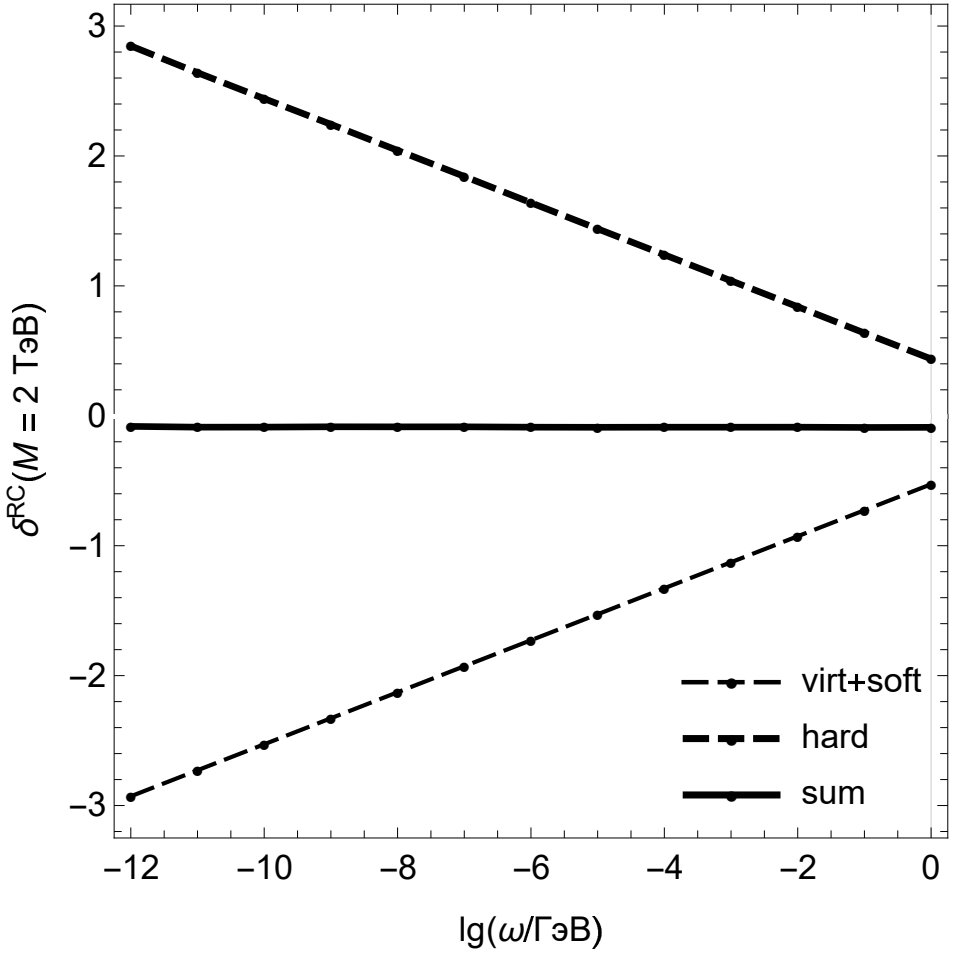

Figure 9: The relative corrections δ^{RC} to differential cross section $\frac{d\sigma}{dM}$ (virtual and soft, hard, their sum) via ω (M=2 TeV).

Relative correction definition:

$$\delta^{\mathrm{RC}}(M) = \frac{d\sigma^{\gamma\gamma}_{\mathrm{RC}}/dM}{d\sigma^{\gamma\gamma}_{0}/dM}.$$

ElectoMagnetic corrections to diff. cross section $d\sigma/dM$

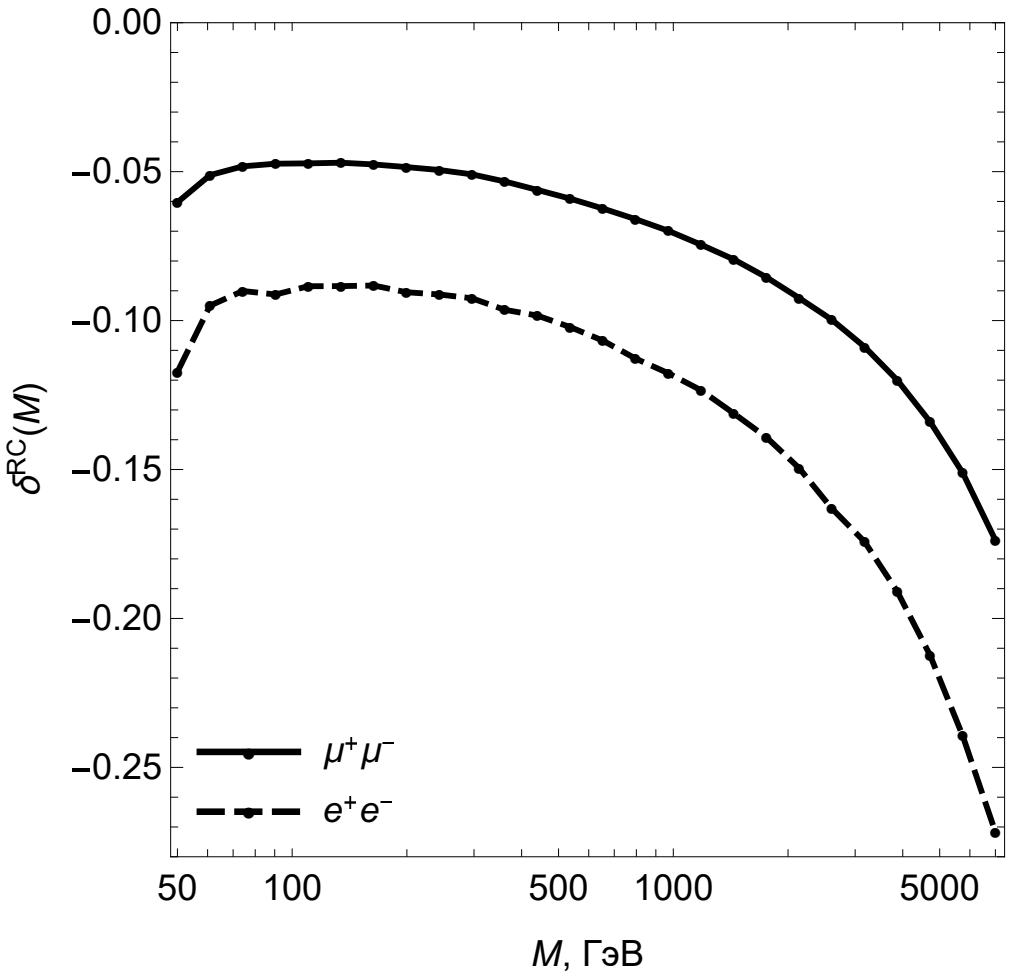

Figure 10: Total relative electromagnetic corrections $\delta^{\mathrm{RC}}(M)$ via M.

ElectoMagnetic corrections to double diff. cross section

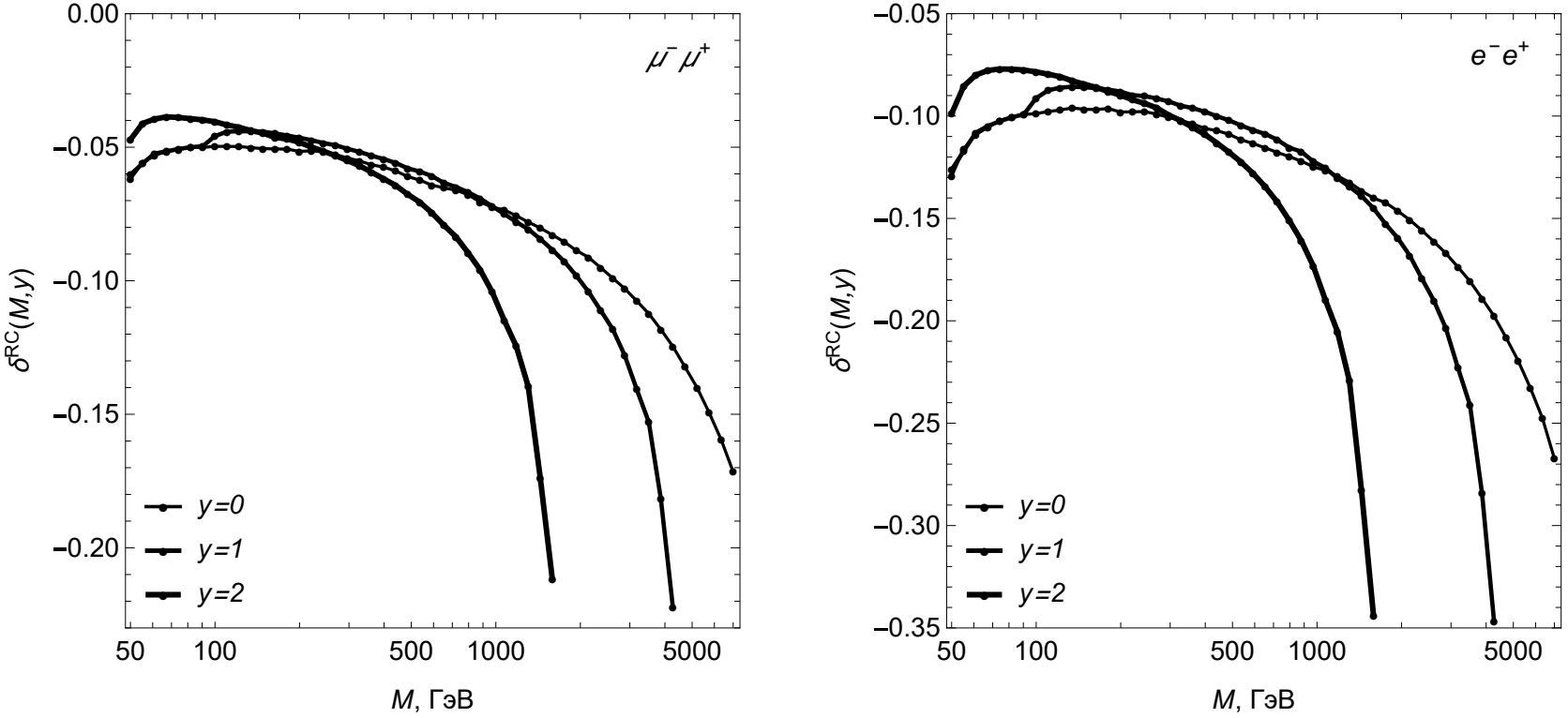

Figure 11: Total relative electromagnetic corrections $\delta^{\mathrm{RC}}(M,y)$ to $\frac{d^2\sigma_0}{dMdy}$ via M at different y.

ElectoWeak corrections to $\frac{d\sigma_0}{dM}$ and $\frac{d^2\sigma_0}{dMdy}$

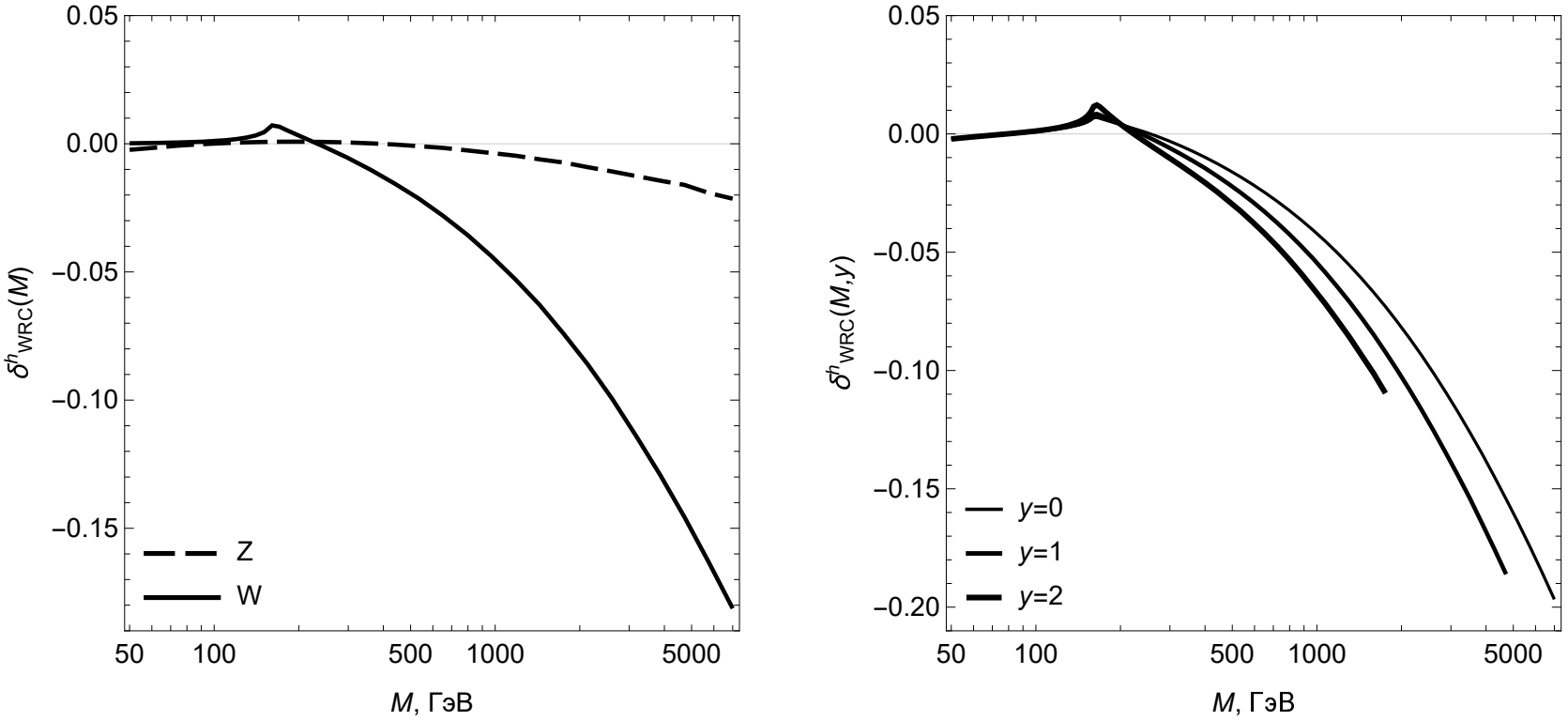

Figure 12: Left (right) – relative electroweak corrections to differential cross section (to double differential cross section at different y) via M.

Total cross sections: standard CMS bins

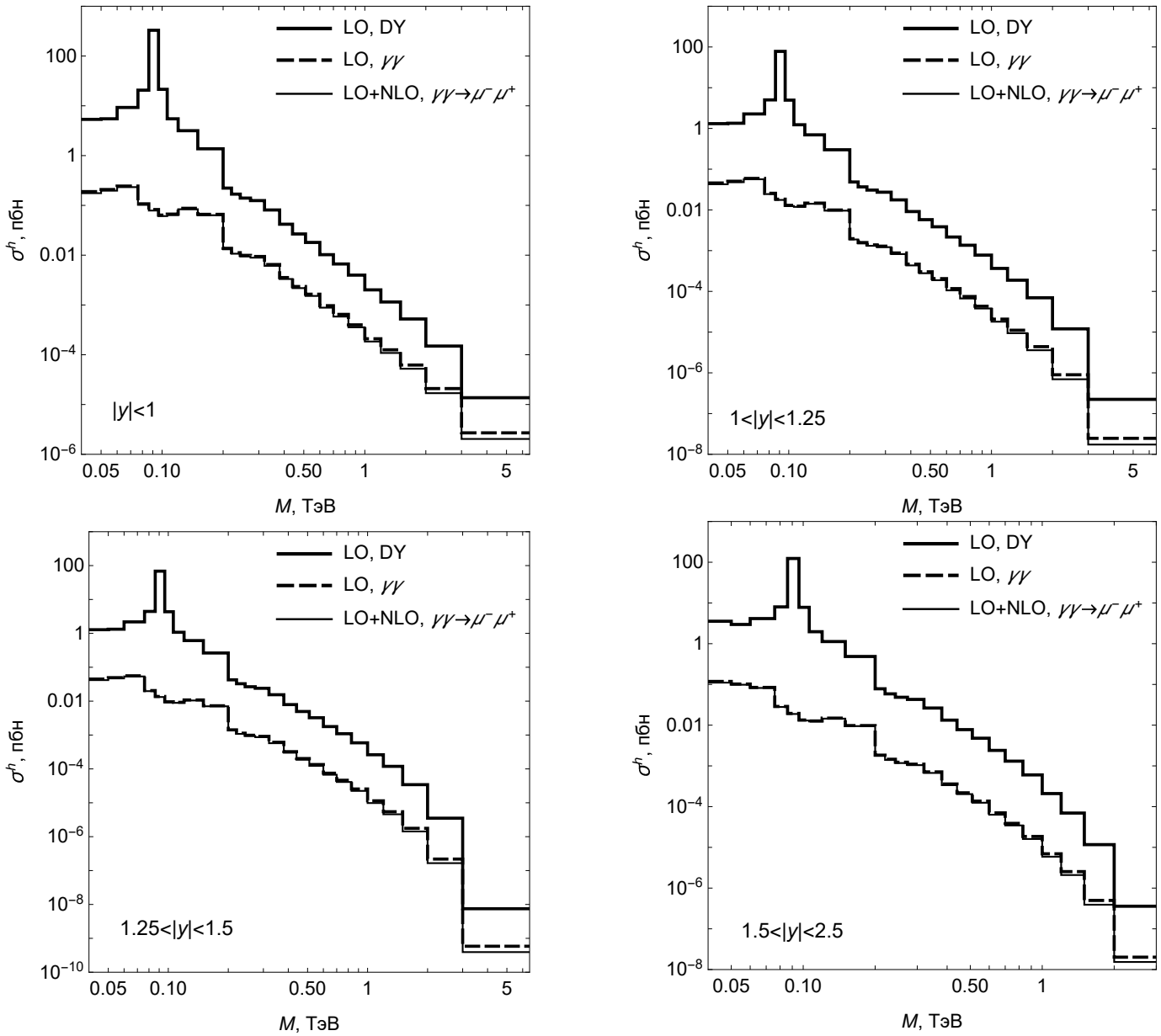

Forward-backward asymmetry

Forward-backward asymmetry $A_{\rm FB}$ is important observable in dilepton production **with a dual nature – electroweak and kinematical**:

$$A_{\rm FB} = \frac{\sigma_{\rm F}^h - \sigma_{\rm B}^h}{\sigma_{\rm F}^h + \sigma_{\rm B}^h}, \tag{12}$$

where according **J. Collins & D. Soper (1977)**:

$\sigma_{\rm F}^h$ is "forward" cross section ($\cos\theta^* > 0$),

$\sigma_{\rm B}^h$ is "backward" cross section ($\cos\theta^* < 0$).

In the Collins–Soper system $\cos\theta^*$ looks like:

$$\cos\theta^* = {\rm sgn}[x_2(t+u_1) - x_1(t_1+u)]\frac{tt_1 - uu_1}{M\sqrt{s(u+t_1)(u_1+t)}}.$$

Forward, Backward (and Experimental) borders

For the case of nonradiative kinematics the $\cos\theta^*$ has especially simple view:

$$\cos\theta^* = \mathrm{sgn}[x_1 - x_2]\frac{u-t}{s} = \mathrm{sgn}\left[e^y - e^{-y}\right]\frac{(1+\mathcal{C})e^{-y} - (1-\mathcal{C})e^y}{(1+\mathcal{C})e^{-y} + (1-\mathcal{C})e^y}.$$

Solving $\cos\theta^* = 0$ we get **two conditions** for border dividing the regions of σ^h_{F} and σ^h_{B}:

$$y = 0, \quad \mathcal{C} \equiv \cos\theta = \mathrm{th}\, y.$$

The CMS experimental condition $|\cos\theta| < \zeta^*$ is trivial but the second one $|\cos\alpha| < \zeta^*$ is rather sophisticated:

$$\cos\left(\arccos\frac{\cos\theta - \mathrm{th}\, y}{r} + \arcsin\frac{\sin\theta\,\mathrm{th}\, y}{r}\right) = \pm\xi^*,$$

where

$$r = \sqrt{1 - 2\cos\theta\,\mathrm{th}\, y + \mathrm{th}^2\, y}.$$

Forward, Backward (and Experimental) regions

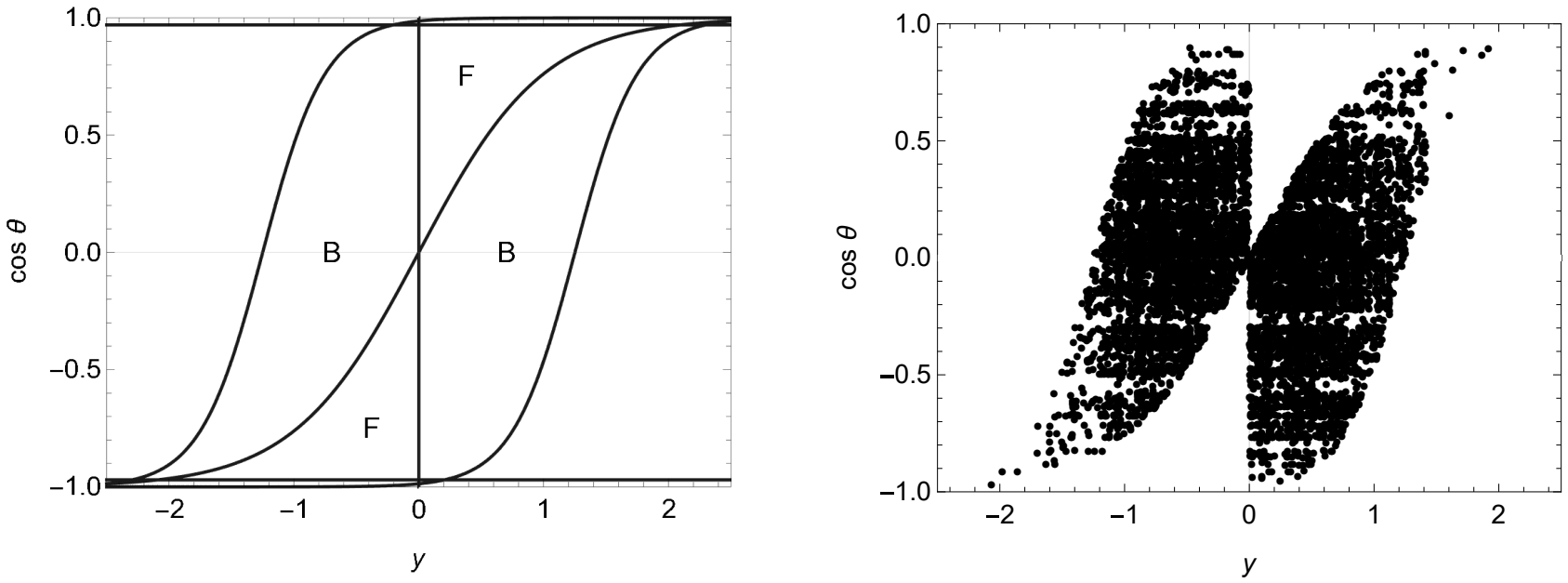

Figure 14: Left – Forward, Backward and CMS regions in y and $\cos\theta$ variables (**borders are**: $y = 0$, $\cos\theta = \mathrm{th}\, y$, $\cos\theta = \pm\zeta^*$, and $\cos\alpha = \pm\zeta^*$, where $\zeta^* \approx 0.9866$),
right – the points sampled by Monte-Carlo generator of VEGAS **for Backward CMS region**.

Interplay of DY and $\gamma\gamma$ for A_{FB}: numerical effect

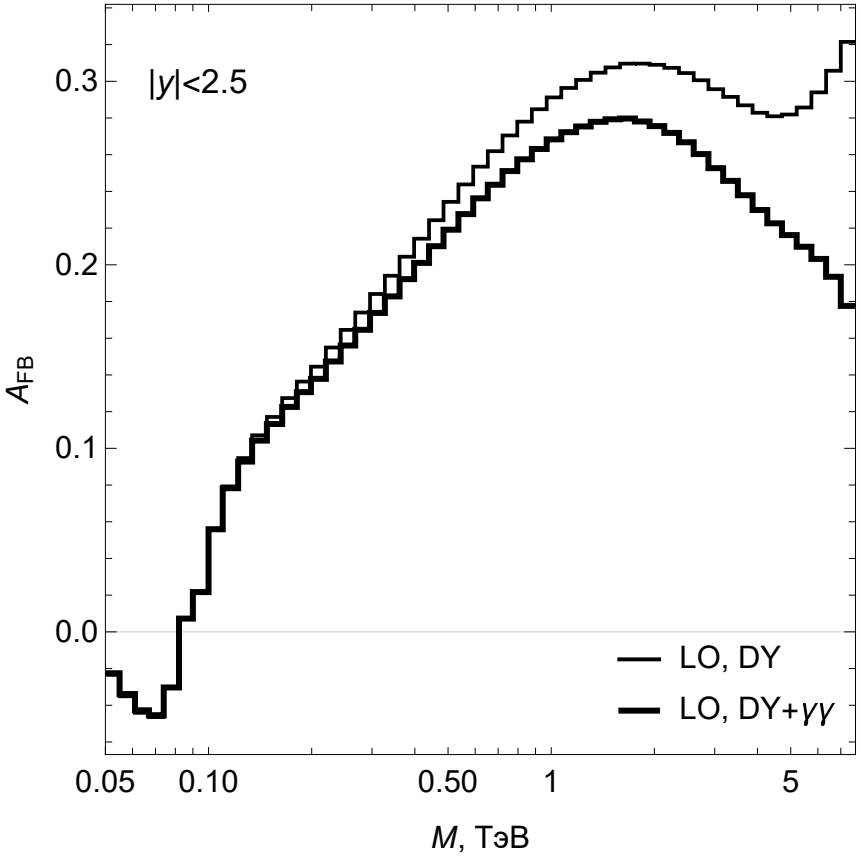

Figure 15: The Born forward-backward asymmetry via M at CMS LHC setup: for **Drell–Yan mechanism** – thin line, for **both mechanisms** (DY and $\gamma\gamma$-fusion) – thick line.

Interplay of DY and $\gamma\gamma$ for $A_{\rm FB}$: explanation

As the Born process $\gamma\gamma$-fusion has **pure electromagnetic nature**, then

$$A_{\rm FB}^{\gamma\gamma} = 0.$$

Therefore the F- an B- cross section are equal:

$$\sigma_{\rm F}^{\gamma\gamma} = \sigma_{\rm B}^{\gamma\gamma} = \Delta.$$

The $\gamma\gamma$-fusion cross section has the scale comparable with DY one **at large** M **region**. Expanding the net asymmetry (DY+$\gamma\gamma$) in series on Δ we get:

$$A_{\rm FB}^{\rm DY+\gamma\gamma} \approx A_{\rm FB}^{\rm DY}\left(1 - \frac{2\Delta}{\sigma_{\rm F+B}^{\rm DY}}\right).$$

This effect (the decreasing of net asymmetry at large M) is well seen in Fig. 15 starting with $M\sim$300 GeV.

A_{FB} for Run3 of CMS LHC: $\mu^+\mu^-$, DY

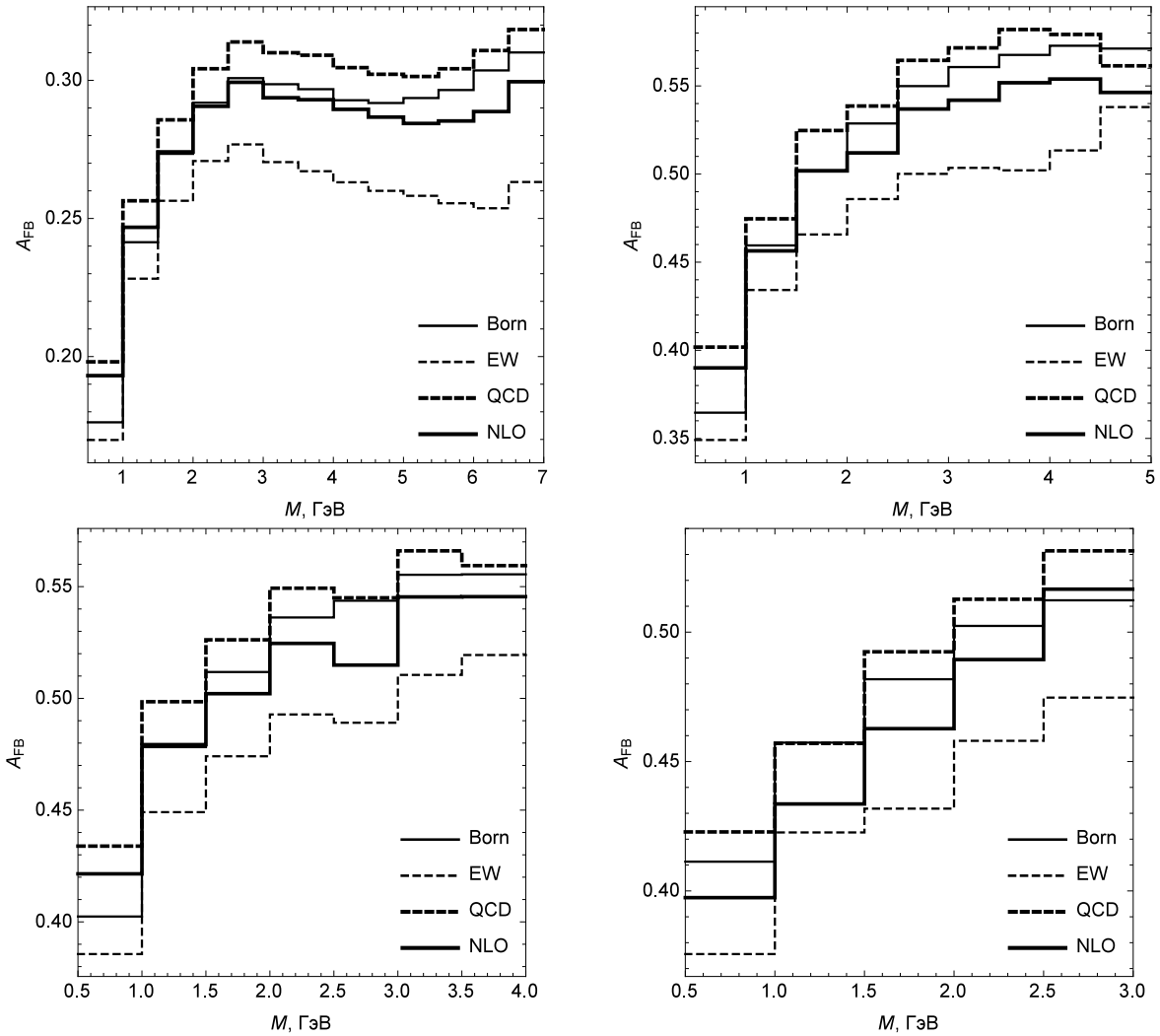

Figure 16: A_{FB} for $\mu^+\mu^-$-production: top – $|y| < 1$ and $1 < |y| < 1.25$, bottom – $1.25 < |y| < 1.5$ and $1.5 < |y| < 2.5$.

A_{FB} for Run3 of CMS LHC: e^+e^-, DY

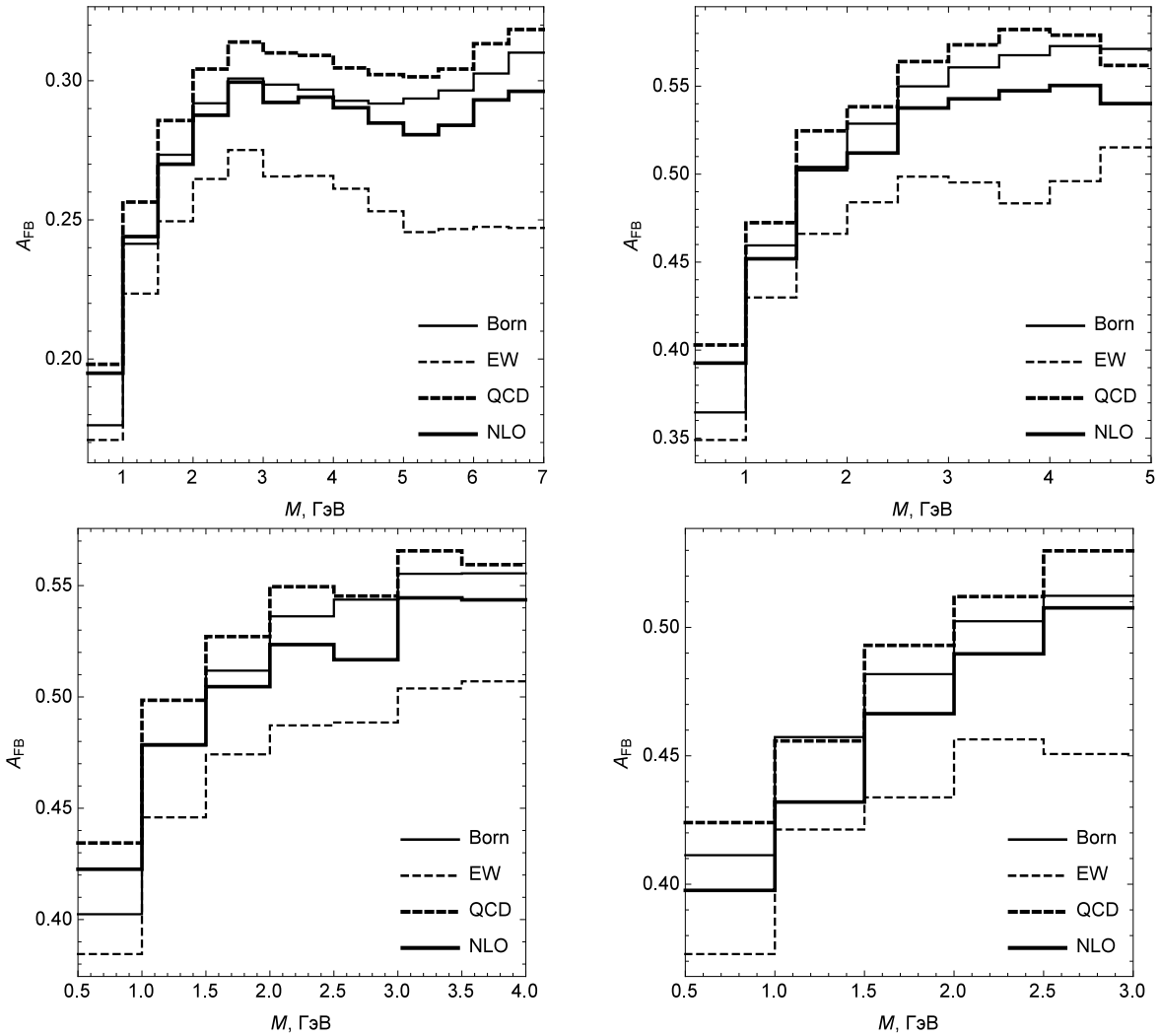

Figure 17: A_{FB} for e^+e^--production: top – $|y| < 1$ and $1 < |y| < 1.25$, bottom – $1.25 < |y| < 1.5$ and $1.5 < |y| < 2.5$.

A_{FB} for Run3 of CMS LHC: $\mu^+\mu^-$, DY and $\gamma\gamma$

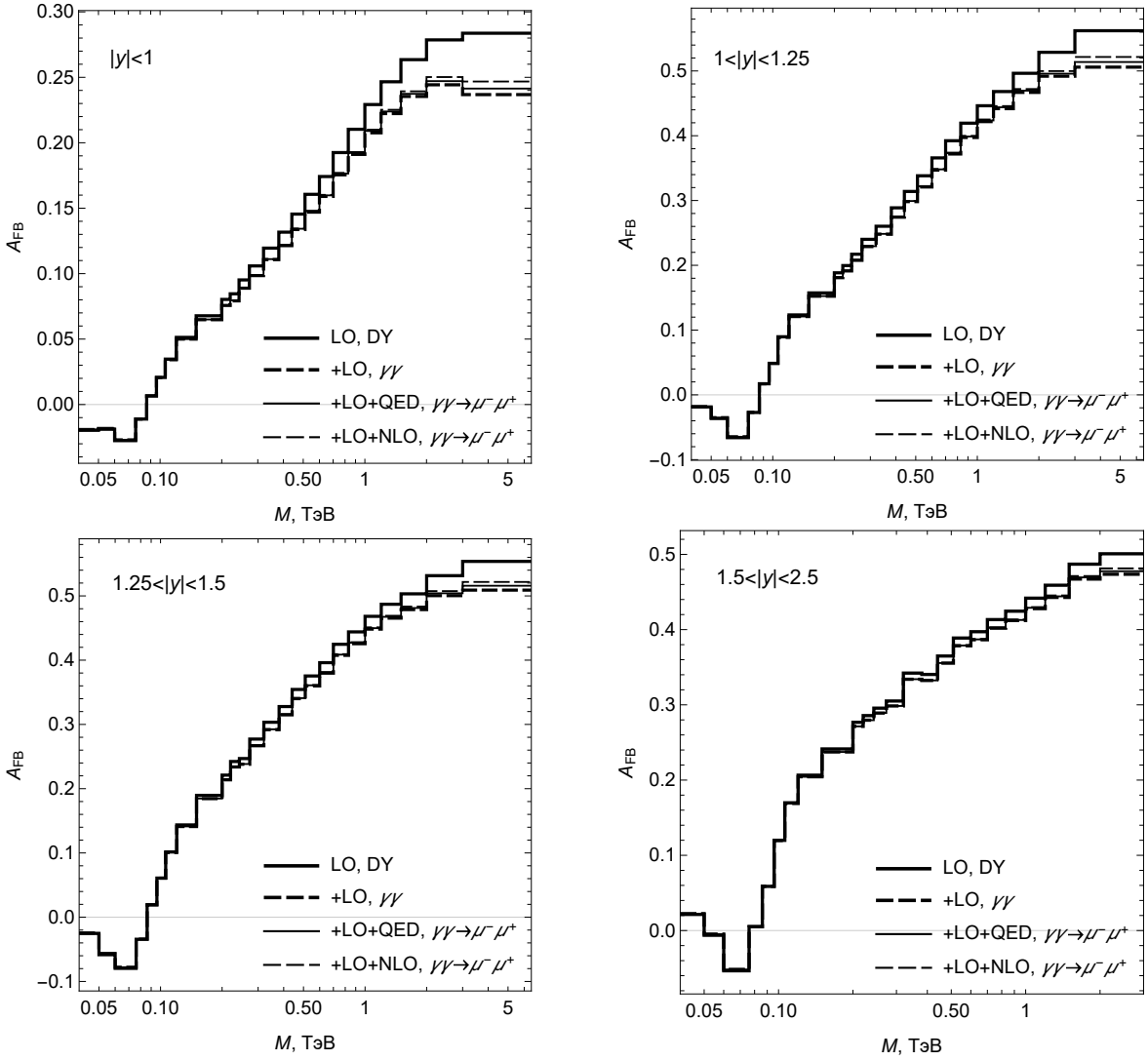

Figure 18: Forward-backward asymmetry A_{FB} for $\mu^+\mu^-$-production.

Conclusions & Acknowledgement

★ **The NLO EWK** corrections to dilepton production with Drell–Yan and $\gamma\gamma$-fusion mechanisms have been studied.

★ It has been ascertained that the considered in Run 3 region radiative corrections change the cross sections and A_{FB} **significantly**.

★ I would like to thank the **RDMS CMS group** members for the stimulating discussions and **CERN (CMS Group)** for warm hospitality during my visits.

★ This work was supported by the **Convergence-2025** Research Program of Republic of Belarus (Microscopic World and Universe Subprogram).

★ The numerical calcualtion was performed partically by **"HybriLIT"** Heterogeneous Platform of the Laboratory of Information Technologies of JINR.